# Microstrip Tri-Mode Bandpass Filters Using Modified Ring Resonators

**Kai-Da Xu[1, 2, *], Yonghong Zhang[2], Jing Ai[2], and Qing Huo Liu[3]**

**Abstract**—Two new microstrip tri-mode modified ring resonators (Resonator A and Resonator B) are presented and discussed through mode analysis method. The characteristic difference between these two resonators is that the center frequency of the tri-mode Resonator B is still the same as that of traditional dual-mode ring resonator, while the center frequency of Resonator A will be shifted up compared with that of traditional ring resonator. Based on these two novel resonators, two bandpass filter examples are designed, fabricated and measured. The simulations and measurements are in good agreement which validate the design ideas.

## 1. INTRODUCTION

For the applications of modern wireless communication systems, numerous different structures developed from the dual mode resonators have been proposed and analyzed intensively to design microstrip single- and multiple-band BPFs [1–8] since Wolff first demonstrated dual-mode resonators in 1972 [9]. Recently, microstrip tri-mode/multi-mode bandpass filters (BPFs) have been extremely attractive due to their advantages of the compact overall sizes and high performance [10–17]. By etching two pairs of rectangular slots on a circular patch resonator to split a pair of fundamental degenerate modes and perturb a third mode, a tri-mode bandpass filter was proposed in [13]. In addition, the tri-mode resonator could be also developed from the loop dual-mode resonator [14, 15], where the new created resonant mode was declined to approach the first two inherent degenerate modes by introducing appropriate perturbation. In [16, 17], the tri-mode resonators were realized by adding a radial-line stub or stepped-impedance line based on a conventional dual-mode stub-loaded resonator.

Using mode analysis method, in this paper, two novel modified tri-mode ring resonators are designed based on the traditional dual-mode ring resonators. Finally, two tri-mode bandpass filter examples using these two resonators, respectively, are simulated, fabricated and measured with high selectivity to validate the design ideas successfully.

## 2. MODIFIED TRI-MODE RING RESONATORS

Figure 1 shows the structures of these two microstrip modified tri-mode ring resonators, Resonator A and Resonator B. Resonator A consists of a traditional ring resonator, two 90°-crossed strips, and four concentric radial stubs loaded to the center of the ring. Resonator B is composed of a traditional ring resonator, a 45°-tilted strip, and three dual E-shaped stubs loaded to the strip.
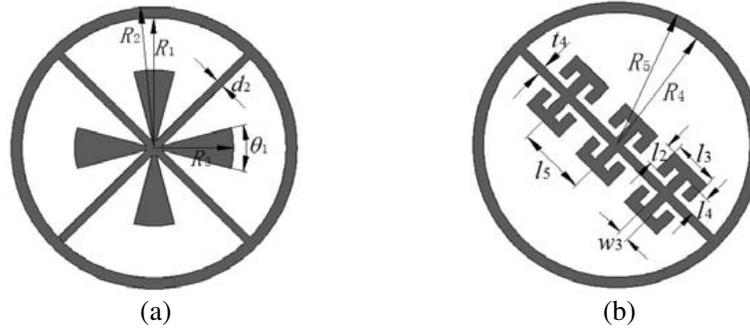
**Figure 1.** Layouts of two modified tri-mode ring resonators: (a) Resonator A: modified ring resonator with radial stub-loaded 90°-crossed strips, and (b) Resonator B: modified ring resonator with a 45°-tilted strip and three dual E-stubs.

## 2.1. Resonator A

To facilitate the illustration of the proposed tri-mode Resonator A, Figure 2 shows three microstrip resonator types of the design process. For a traditional microstrip ring resonator (Type 1) as shown in Figure 2(a), the fundamental resonance occurs when the guided wavelength $\lambda_g$ is identical to the perimeter of the ring [18, 19], whose resonant frequency satisfies the following equation,

$$f = \frac{c}{\lambda_g \sqrt{\varepsilon_{eff}}} \tag{1}$$

where $c$ is the velocity of light in free space, and $\varepsilon_{eff}$ denotes the effective dielectric constant of the substrate. The higher resonant modes are theoretically located at any multiple of the fundamental resonance. As tabulated in Table 1, the two first-order degenerate modes (Mode 1 and Mode 2) are excited and their resonant frequencies are almost the same. Mode 3 and Mode 4 of the Resonator Type 1 are also degenerate modes, whose resonant frequencies are close to each other as well as approximately twice of the Mode 1 or Mode 2.

When two 90°-crossed strips are connected to the ring resonator as illustrated in Figure 2(b), an additional mode will be generated among the first pair of degenerate modes and the second pair of ones, which is Mode 3 of Type 2 in Table 1. Meanwhile, the first pair of degenerate modes is slightly shifted up comparing with that of Resonator Type 1. In order to make the third mode approach the first two modes as close as possible to obtain a tri-mode resonator BPF with good passband selectivity, as shown in Figure 2(c), four concentric radial stubs are loaded to the center of the ring resonator based on the Type 2 of Figure 2(b). Consequently, the resonant frequencies of the first three modes become
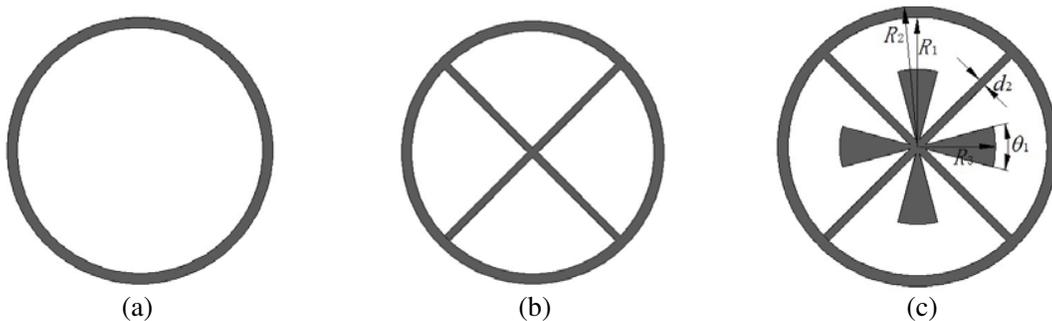


**Figure 2.** Layouts of three resonators in the design process for Resonator A: (a) traditional ring resonator, Type 1, (b) the ring resonator with 90°-crossed strips, Type 2, and (c) modified ring resonator with radial stub-loaded 90°-crossed strips, Type 3.

3.86 GHz, 3.95 GHz, and 3.97 GHz, respectively, which are very close to each other as shown in Type 3 of the Table 1.

Note that the values of resonant frequencies in Table 1 can be easily obtained by any commercial full-wave electromagnetic eigenmode simulation. To compare the differences of the characteristics among these three resonator types, they are designed on the same substrate with a relative dielectric constant

**Table 1.** Resonant frequencies of the first five modes of three corresponding resonators in Figure 2.

| Types (Physical dimensions) / Resonant modes | Type 1 ($R_1 = 8.3$ mm, $R_2 = 9$ mm) | Type 2 ($R_1 = 8.3$ mm, $R_2 = 9$ mm, $d_2 = 0.5$ mm) | Type 3 ($R_1 = 8.3$ mm, $R_2 = 9$ mm, $R_3 = 5$ mm, $d_2 = 0.5$ mm, $\theta1 = 14.5°$) |
|---|---|---|---|
| Mode 1 | 2.99 GHz | 3.45 GHz | 3.86 GHz |
| Mode 2 | 3.03 GHz | 3.53 GHz | 3.95 GHz |
| Mode 3 | 6.00 GHz | 5.67 GHz | 3.97 GHz |
| Mode 4 | 6.15 GHz | 5.94 GHz | 5.69 GHz |
| Mode 5 | 9.31 GHz | 6.19 GHz | 5.73 GHz |



(a)          (b)
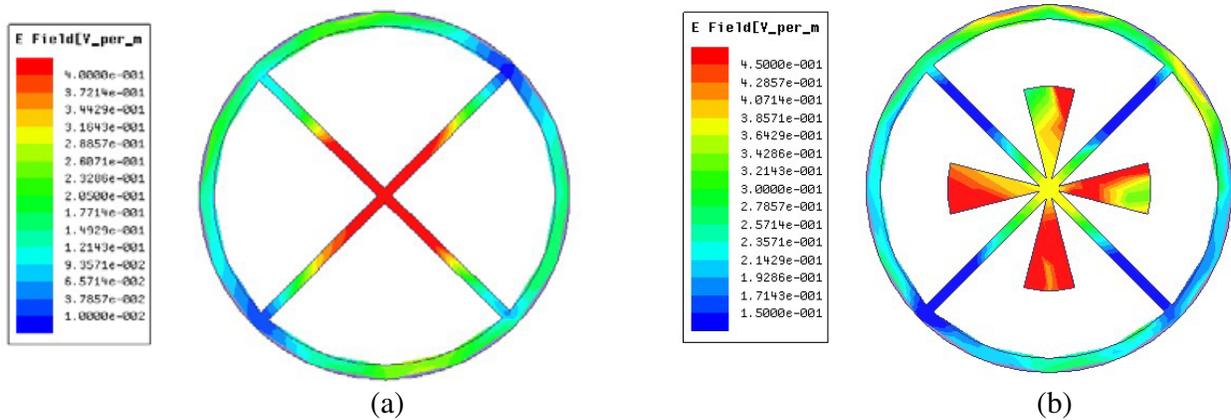
**Figure 3.** Simulated electric field magnitude distribution of the Mode 3: (a) at 5.67 GHz of Type 2, and (b) at 3.97 GHz of Type 3.
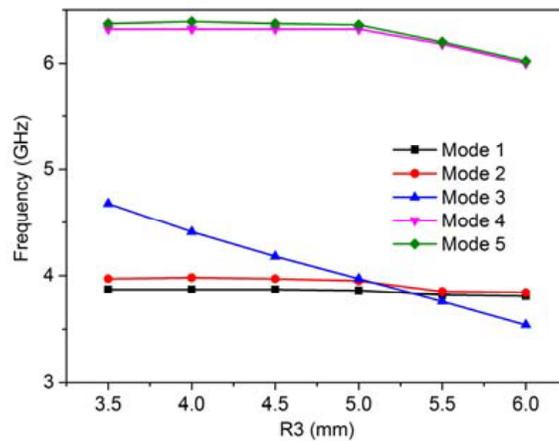


**Figure 4.** Simulated resonant frequencies of the first five modes with varying $R_3$ for Resonator Type 3.

of 3.5 and a thickness of 0.508 mm. In addition, same physical dimensions are set as shown in Table 1. Figure 3 shows the simulated $E$-field magnitude distribution of the third mode in the Resonators Type 2 and Type 3. At 5.67 GHz of the Type 2, the maximum $E$-field distributes in the center of the resonator as shown in Figure 3(a), while at 3.97 GHz for the third mode of the Type 3, the maximum $E$-field distribution transfers to locate at the four radial stubs instead of the resonator center. Moreover, only Mode 3 of the first five resonant modes has the maximum $E$-field at the resonator center for the Type 2. Therefore, the third mode resonant frequency of the Type 3 is only dependent on the dimensions of the four radial stubs. If we fix the angle $\theta 1 = 14.5°$ but change the radius of the radial stub $R_3$, as depicted in Figure 4, the resonant frequencies of the first two modes are almost unchangeable while Mode 3 is varied with the radius of the radial-line stubs, whose resonant frequency is shifted down from 4.68 GHz to 3.54 GHz as the radius of the radial stub increases from 3.5 mm to 6 mm. We can conclude that the first pair of degenerate modes as well as the third mode of the proposed resonator can be obtained independently by adjusting the radii of the ring and radial stubs, respectively.

## 2.2. Resonator B

Similarly, Figure 5 shows another four resonator types to facilitate the design process illustration of the proposed Resonator B, which are also designed on the aforementioned substrate. The parameters of these four resonators shown in Figure 5(d) are set as $R_4 = 7.5$ mm, $R_5 = 8.1$ mm, $t_4 = 0.5$ mm, $w_3 = 0.6$ mm, $l_2 = 1.4$ mm, $l_3 = 2.6$ mm, $l_4 = 1.2$ mm, and $l_5 = 4.8$ mm. The proposed modified tri-mode ring Resonator B (Type 4') consists of a traditional ring resonator and a 45°-tilted strip loaded with three dual E-shaped stubs.
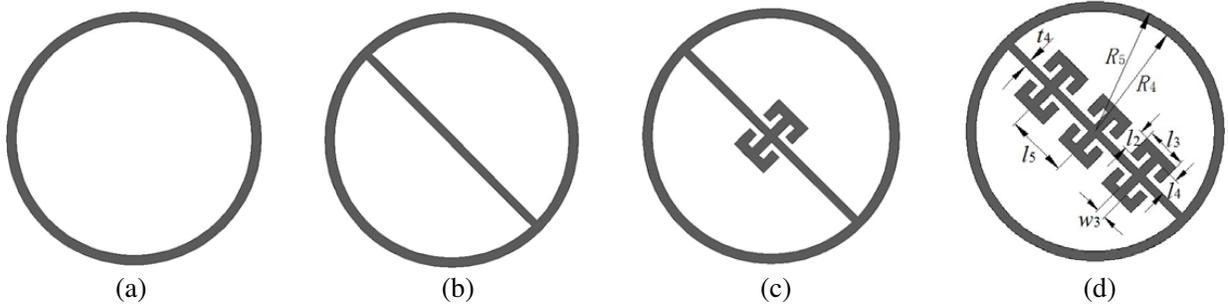


**Figure 5.** Layouts of four resonators in the design process for Resonator B: (a) traditional ring resonator, Type 1', (b) the ring resonator with a 45°-tilted strip, Type 2', (c) the ring resonator with a 45°-tilted strip and a dual E-stub, Type 3', and (d) modified ring resonator with a 45°-tilted strip and three dual E-stubs, Type 4'.

Table 2 shows the resonant frequencies of the first five modes of the four corresponding resonators of Figure 5. When a 45°-tilted strip is connected to the traditional ring resonator as illustrated in Figure 5(b), an additional mode will be generated among the first pair of degenerate modes and the second pair of ones, which is the Mode 3 of Type 2' in Table 2. In order to make the third mode close to the first two modes, a dual E-shaped stub is loaded to the center of the strip as shown in Figure 5(c). When two other dual E-stubs are added based on the Resonator Type 3', the first three modes of the Resonator Type 4' are closer, whose resonant frequencies become 3.59 GHz, 3.64 GHz, and 3.69 GHz, respectively.

Note that the first mode (Mode 1) almost keeps unchanged but Mode 3 decreases when the traditional ring resonator transfers to the proposed modified resonator, while Mode 2 is shifted up and then down to the original value again. This characteristic is quite different from Resonator A, where Modes 1 and 2 are both shifted up to approach Mode 3 and simultaneously Mode 3 decreases for the process from traditional ring resonator to Resonator A. It means the center frequency of the tri-mode Resonator B is still the same as that of initial dual-mode ring resonator (Type 1'), while the center frequency of the tri-mode Resonator A cannot keep fixed. Figure 6 shows the comparison of resonant frequency points between the initial dual-mode ring resonator and the proposed Resonator B

**Table 2.** Resonant frequencies of the first five modes of four corresponding resonators in Figure 5.

| Types (Physical dimensions, unit: mm) / Resonant modes | Type 1' ($R_4 = 7.5$, $R_5 = 8.1$) | Type 2' ($R_4 = 7.5$, $R_5 = 8.1$, $t_4 = 0.5$) | Type 3' ($R_4 = 7.5$, $R_5 = 8.1$, $t_4 = 0.5$, $w_3 = 0.6$, $l_2 = 1.4$, $l_3 = 2.6$, $l_4 = 1.2$) | Type 4' ($R_4 = 7.5$, $R_5 = 8.1$, $t_4 = 0.5$, $w_3 = 0.6$, $l_2 = 1.4$, $l_3 = 2.6$, $l_4 = 1.2$, $l_5 = 4.8$) |
|---|---|---|---|---|
| Mode 1 | 3.57 GHz | 3.58 GHz | 3.59 GHz | 3.59 GHz |
| Mode 2 | 3.63 GHz | 4.16 GHz | 3.90 GHz | 3.64 GHz |
| Mode 3 | 7.01 GHz | 4.98 GHz | 4.01 GHz | 3.69 GHz |
| Mode 4 | 7.08 GHz | 6.32 GHz | 6.32 GHz | 6.30 GHz |
| Mode 5 | 10.21 GHz | 7.09 GHz | 6.96 GHz | 6.43 GHz |
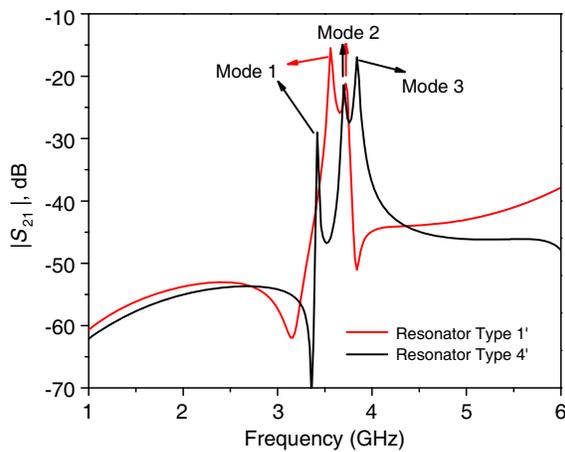


**Figure 6.** Simulated insertion losses of the traditional ring resonator and the proposed Resonator B under weak coupling.
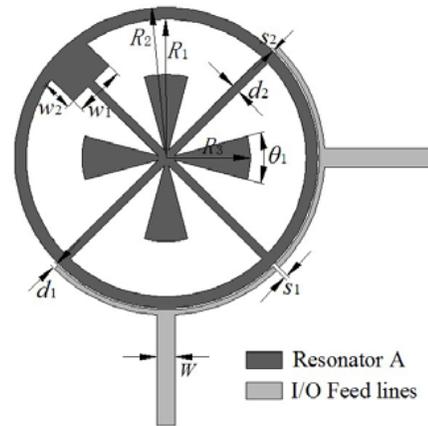


**Figure 7.** Schematic diagram of the proposed Filter A.

under weak coupling. In contrast to the Resonator Type 1', Modes 1 and 2 of the Resonator Type 4' almost keep unchanged, and Mode 3 is moved close to the first two modes. With this unique property, therefore, it is quite convenient for the triple mode filter design using Resonator B because the center frequency of the filter also satisfies Equation (1), which means that the center frequency of this tri-mode filter is only dependent on that of the conventional ring resonator.

## 3. TRI-MODE BPFS USING MODIFIED RING RESONATORS

On the basis of the proposed modified tri-mode ring Resonators A and B, two bandpass filters have been fabricated and implemented on the aforementioned substrate.

### 3.1. Tri-Mode Filter A: BPF Using Resonator A

Figure 7 depicts the layout of a microstrip tri-mode BPF using Resonator A. The characteristic impedances of the microstrip input/output (I/O) feed lines are taken as 50 Ohms. A square patch with size $w_1 \times w_2$ is used to create a small perturbation for the degenerate mode frequency split. The dimensions shown in Figure 7 are chosen as follows: $\theta_1 = 14.5°$, $R_1 = 8.3$ mm, $R_2 = 9$ mm, $R_3 = 5$ mm, $d_1 = 0.3$ mm, $d_2 = 0.5$ mm, $w_1 = 3$ mm, $w_2 = 1.9$ mm, $s_1 = 0.2$ mm, $s_2 = 0.1$ mm, $W = 1.1$ mm.

The simulation and measurement are accomplished by using HFSS software [20] and network analyzer, respectively. As shown in Figure 8, the measured results are in good agreement with the full-wave simulated ones. The measured 3 dB bandwidth of the BPF is found to be 280 MHz (7.3%) with
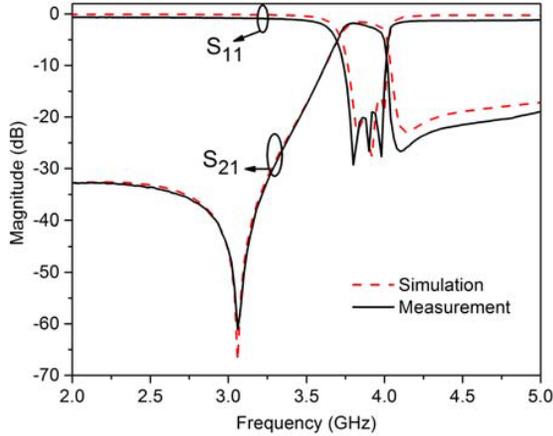
**Figure 8.** Simulated and measured frequency responses of the proposed Filter A.
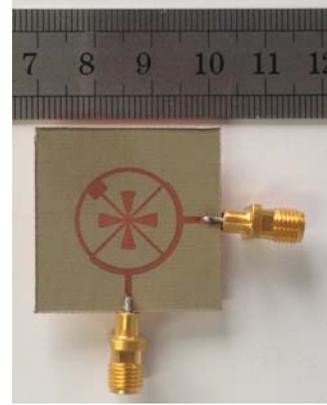


**Figure 9.** Photograph of the fabricated Filter A.

the center frequency of 3.84 GHz. The insertion losses, including the losses from two SMA connectors, are around 1.8 dB at the passband, and the return losses within the passband are above 19 dB. Two transmission zeros are located at 3.06 and 4.1 GHz. The photograph of the fabricated Filter A can be seen in Figure 9.

### 3.2. Tri-mode Filter B: BPF Using Resonator B

Figure 10(a) shows the schematic diagram of the tri-mode BPF using the proposed Resonator B. The characteristic impedances of the microstrip I/O feed lines are also taken as 50 Ohms. The dimensions are chosen as follows: $t_1 = t_2 = 0.1$ mm, $t_3 = t_4 = 0.5$ mm, $W = 1.1$ mm, $w_3 = 0.6$ mm, $R_4 = 7.5$ mm, $R_5 = 8.1$ mm, $l_1 = 3.5$ mm, $l_2 = 1.4$ mm, $l_3 = 2.6$ mm, $l_4 = 1.2$ mm, and $l_5 = 3.9$ mm. To improve the performance of the filter, the technique of source-load cross coupling is adopted to generate an additional transmission zero. Therefore, there are three transmission zeros of this BPF including two inherently generated transmission zeros located at each side of the passband symmetrically as shown in Figure 11.

   The coupling scheme of this tri-mode filter is illustrated in Figure 10(b). The dark and white circles represent resonant modes and source/load, respectively. The dashed line indicates the cross coupling between source and load that is dominantly determined by the gap value $t_1$ and length value $l_1$. The coupling strength between the resonator and source/load can be also controlled by changing the gap value $t_2$. Due to the symmetry of the filter layout, the corresponding coupling matrix of the coupling



(a)                                                                              (b)
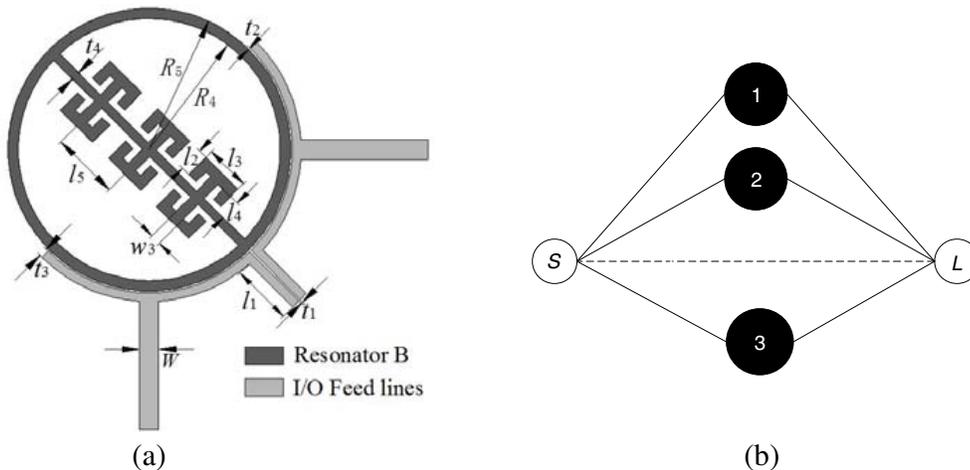
**Figure 10.** (a) Schematic diagram, and (b) coupling scheme of the proposed Filter B.
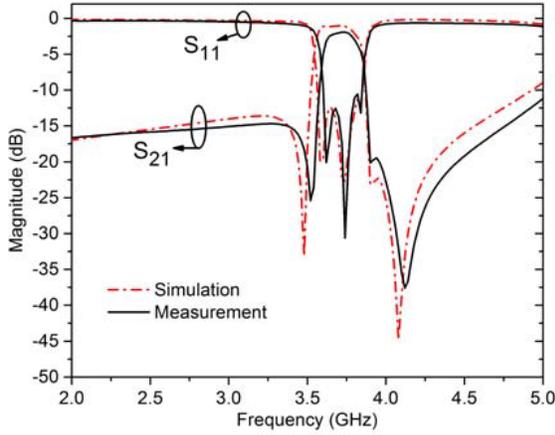
**Figure 11.** Simulated and measured frequency responses of the proposed Filter B.
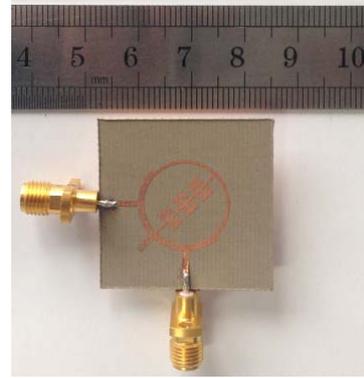


**Figure 12.** Photograph of the fabricated Filter B.

**Table 3.** Performance comparison of some reported tri-mode BPFs.

| Reference | $\varepsilon_r/h$ (mm) of substrate | Center frequency (GHz) | 3-dB FBW (%) | Return loss/ Insert loss (dB) | Number of transmission zeros | Circuit size (mm$^2$) ($\lambda_g \times \lambda_g$) |
|---|---|---|---|---|---|---|
| [13] | 10.2/0.635 | 2.42 | 28.8 | 16/0.5 | 0 | 16.2 × 16.2 (0.52 × 0.52) |
| [14] | 9.2/1.0 | 2.4 | 4.79 | 17/2.4 | 3 | 20 × 17.3 (0.62 × 0.53) |
| [15] | 2.65/0.5 | 3.78 | 4 | 19.9/2.9 | 3 | 18.4 × 18.4 (0.34 × 0.34) |
| Filter B of this work | 3.5/0.508 | 3.7 | 7 | 11/1.7 | 3 | 16 × 16 (0.33 × 0.33) |

scheme is given by

$$
M = \begin{bmatrix}
0 & M_{S1} & M_{S2} & M_{S3} & M_{SL} \\
M_{S1} & M_{11} & 0 & 0 & M_{1L} \\
M_{S2} & 0 & M_{22} & 0 & M_{2L} \\
M_{S3} & 0 & 0 & M_{33} & M_{3L} \\
M_{SL} & M_{1L} & M_{2L} & M_{3L} & 0
\end{bmatrix}
\tag{2}
$$

The measured results of $S$-parameters are in good agreement with the simulated ones as exhibited in Figure 11. The measurement shows that the 3 dB bandwidth is 260 MHz (7%) with the center frequency of 3.7 GHz. The insertion losses, including the losses from two SMA connectors, are about 1.7 dB in the passband, and the return losses are better than 11 dB. There are three transmission zeros located at 3.52, 3.9, and 4.12 GHz, respectively. Figure 12 is the photograph of the fabricated Filter B. Its size amounts to 16 mm × 16 mm $(0.33\lambda_g \times 0.33\lambda_g)$, where $\lambda_g$ is the guided wavelength of 50 Ohm microstrip line at 3.7 GHz. Table 3 summarized the comparisons of the proposed Filter B with other reported tri-mode filters in recent years.

## 4. CONCLUSION

In this paper, two tri-mode resonators have been proposed and discussed through mode analysis method. Then, these two resonators are applied in the required two bandpass filters, respectively. The proposed design structures are verified by the fabrications and measurements of the filters, where both of the measured results agree well with the simulated ones. In contrast to Resonator A, Resonator B is

more convenient for the tri-mode filter design because the center frequency of the tri-mode filter using Resonator B is only dependent on that of the traditional dual-mode ring resonator.

## REFERENCES

1. Hong, J. S. and S. Li, "Theory and experiment of dual-mode microstrip triangular patch resonators and filters," *IEEE Trans. Microw. Theory Tech.*, Vol. 52, No. 3, 1237–1243, 2004.

2. Mao, R. J. and X. H. Tang, "Novel dual-mode bandpass filters using hexagonal loop resonators," *IEEE Trans. Microw. Theory Tech.*, Vol. 54, No. 9, 3526–3533, 2006.

3. Xu, K. D., Y. H. Zhang, C. L. Zhuge, and Y. Fan, "Miniaturized dual-band bandpass filter using short stub-loaded dual-mode resonators," *Journal of Electromagnetic Waves and Applications*, Vol. 25, No. 16, 2264–2273, 2011.

4. Tu, W.-H., "Compact double-mode cross-coupled microstrip bandpass filter with tunable transmission zeros," *IET Microw. Antennas Propag.*, Vol. 2, No. 4, 373–377, 2008.

5. Xu, K. D., Y. H. Zhang, Y. Fan, W. T. Joines, and Q. H. Liu, "Novel circular dual-mode filter with both capacitive and inductive source-load coupling for multiple transmission zeros," *Journal of Electromagnetic Waves and Applications*, Vol. 26, No. 13, 1675–1684, 2012.

6. Sun, S., "A dual-band bandpass filter using a single dual-mode ring resonator," *IEEE Microw. Wirel. Compon. Lett.*, Vol. 21, No. 6, 298–300, 2011.

7. Xu, K. D., Y. H. Zhang, W. T. Joines, Q. H. Liu, and Y. Fan, "Tri-band bandpass filter using short stub-loaded dual-mode resonators," *Microw. J.*, Vol. 56, No. 9, 122–130, 2013.

8. Xu, K. D., Y. H. Zhang, Y. Fan, W. T. Joines, and Q. H. Liu, "Microstrip dual-mode bandpass filter design using pie-section truncated semi-circle and quarter-circle resonators," *IET Microw. Antennas Propag.*, Vol. 9, No. 3, 224–229, 2015.

9. Wolff, I., "Microstrip bandpass filter using degenerate modes of a microstrip ring resonator," *Electron. Lett.*, Vol. 8, 302–303, 1972.

10. Tu, W. H., "Microstrip bandpass filters using cross-shaped triple-mode resonator," *IET Microw. Antennas Propag.*, Vol. 4, No. 9, 1421–1426, 2010.

11. Chen, F. C., Q. X. Chu, Z. H. Li, and X. H. Wu, "Compact dual-band bandpass filter with controllable bandwidths using stub-loaded multiple-mode resonator," *IET Microw. Antennas Propag.*, Vol. 6, No. 10, 1172–1178, 2012.

12. Lee, K. C., H. T. Su, and M. K. Haldar, "Compact quadruple-mode resonator for wideband bandpass filter design," *IET Microw. Antennas Propag.*, Vol. 8, No. 2, 67–72, 2014.

13. Serrano, A. L. C. and F. S. Correra, "A triple-mode bandpass filter using a modified circular patch resonator," *Microw. Opt. Technol. Lett.*, Vol. 51, No. 1, 178–182, 2009.

14. Mo, S.-G., Z.-Y. Yu, and L. Zhang, "Design of triple-mode bandpass filter using improved hexagonal loop resonator," *Progress In Electromagnetics Research*, Vol. 96, 117–125, 2009.

15. Wei, C. L., B. F. Jia, and Z. J. Zhu, "Design of triple-mode microstrip filter with source-load coupling," *Microw. Opt. Technol. Lett.*, Vol. 53, No. 10, 2403–2406, 2011.

16. Zhang, L., Z. Y. Yu, and S. G. Mo, "Design of compact triple-mode bandpass filter using double center stubs-loaded resonator," *Microw. Opt. Technol. Lett.*, Vol. 52, No. 9, 2109–2111, 2010.

17. Chen, C. F., "Design of a compact microstrip quint-band filter based on the tri-mode stub-loaded stepped-impedance resonators," *IEEE Microw. Wirel. Compon. Lett.*, Vol. 22, No. 7, 357–359, 2012.

18. Chang, K. and L. H. Hsieh, *Microstrip Ring Circuits and Related Structures*, Wiley, New York, USA, 2004.

19. Xu, K. D., Y. H. Zhang, Y. Fan, J. L. W. Li, W. T. Joines, and Q. H. Liu, "Planar dual- and tri-band bandpass filters using single improved ring resonator and simple feed scheme," *Microw. Opt. Technol. Lett.*, Vol. 56, No. 3, 574–577, 2014.

20. *Ansoft High Frequency Structural Simulator (HFSS)*, 12th edition, Ansoft Corp., Framingham, MA, USA, 2006.